Weierstraß–Institut
für Angewandte Analysis und Stochastik

im Forschungsverbund Berlin e.V.

A posteriori error estimates for elliptic variational inequalities

Ralf Kornhuber

submitted: 15th February 1995

Weierstraß–Institut
für Angewandte Analysis
und Stochastik
Mohrenstraße 39
D – 10117 Berlin
Germany

A Posteriori Error Estimates
for Elliptic Variational Inequalities

Ralf Kornhuber
Weierstraß-Institut für Angewandte Analysis und Stochastik Berlin
Mohrenstraße 39 D–10117 Berlin, Fed. Rep. of Germany

Abstract. We derive a posteriori error estimates for elliptic variational inequalities. The evaluation amounts to the solution of corresponding scalar local subproblems. Upper bounds for the effectivity rates are given. The theoretical considerations are illustrated by numerical experiments.

Zusammenfassung. Wir entwickeln a posteriori Fehlerschätzungen für elliptische Variationsungleichungen. Die Auswertung erfordert die Lösung entsprechender skalarer, lokaler Teilprobleme. Es werden obere Schranken für die Effektivitätsraten angegeben, und wir illustrieren die numerischen Eigenschaften anhand typischer Beispiele.

1 Introduction

A posteriori error estimates play a crucial role in the solution of partial differential equations by adaptive finite element methods. In this paper we will consider hierarchical error estimates which are characterized by consisting of the following two steps

- Discretize the defect problem with respect to an enlarged space.

- Localize the discrete defect problem by domain decomposition.

The first appearance of hierarchical error estimates that we know is in the work of Zienkiewicz et al. [29] in the early eighties. The intimate relation to preconditioning was made explicit by Deuflhard, Leinen and Yserentant [9]. Recently, it turned out that the hierarchical approach allows a unified view on a variety of apparently different concepts (c.f. Bornemann, Erdmann and Kornhuber [4, 5] and Verfürth [27, 28]).

Bank and Smith [3] have extended hierarchical error estimates from the elliptic selfadjoint case to a variety of other situations including smooth nonlinear problems. Here we will concentrate on non–smooth optimization problems as arising in the fixed domain formulation of certain free boundary problems. Obstacle problems or semi–discretized Stefan problems are typical examples. A straightforward extension of hierarchical error estimates from the linear elliptic case to obstacle problems was applied successfully by Kornhuber and Roitzsch [22] to a special problem from semiconductor device simulation. However, it turned out in the subsequent analysis and numerical experiments (c.f. Hoppe and Kornhuber [16]) that in general the resulting local error estimator suffers from a certain lack of robustness. In the present paper this problem is remedied by a suitable choice of the underlying preconditioner. Moreover, our new approach covers a considerably larger class of problems. We derive upper bounds for the effectivity rates which at least in the linear selfadjoint case do not depend on the stepsize. Numerical examples illustrate the efficiency and reliability of the error estimates and of corresponding mesh–refinement strategies.

2 The Continuous Problem and its Discretization

Let Ω be a bounded polygonal domain in the Euclidean space $\mathbb{R}^2$. We consider the optimization problem

$$u \in H_0^1(\Omega): \quad \mathcal{J}(u) + \phi(u) \leq \mathcal{J}(v) + \phi(v), \quad v \in H_0^1(\Omega). \qquad (2.1)$$

Other boundary conditions of Neumann or mixed type and the case of three space dimensions can be treated in a similar way. The quadratic functional

$$\mathcal{J}(v) = \tfrac{1}{2}a(v,v) - \ell(v) \qquad (2.2)$$

is induced by a continuous, symmetric and $H_0^1(\Omega)$–elliptic bilinear form $a(\cdot,\cdot)$ and a linear functional $\ell \in H^{-1}(\Omega)$. The convex functional $\phi : H_0^1(\Omega) \to \mathbb{R} \cup \{+\infty\}$ of the form

$$\phi(v) = \int_\Omega \Phi(v(x))dx, \qquad (2.3)$$

is generated by a scalar convex function Φ. We assume that Φ is chosen in such a way that ϕ is lower semicontinuous and proper in the sense that $\phi \not\equiv \infty$. To fix the ideas, we give two typical examples. The first one is an obstacle problem generated by the indicator functional

$$\Phi(z) = \begin{cases} 0, & \text{if } z \leq \theta_0 \\ \infty, & \text{if } z > \theta_0 \end{cases} \qquad (2.4)$$

with some fixed upper obstacle $\theta_0 \in \mathbb{R}$. The other example is resulting from the implicit time discretization of two–phase Stefan problems. Here the piecewise quadratic function of the form

$$\Phi(z) = \tfrac{1}{2}a_1(z - \theta_0)^2 - s_1(z - \theta_0) + \tfrac{1}{2}a_2(z - \theta_0)^2 - s_2(z - \theta_0) \qquad (2.5)$$

with suitable constants $a_1, a_2, s_1, s_2 \in \mathbb{R}$ is the potential of the generalized enthalpy. Note that a jump of the derivative occurs at the phase transition temperature $\theta_0 \in \mathbb{R}$. For a variety of further examples, we refer to Crank [8], Duvaut and Lions [11] and others.

It is well–known (c.f. Glowinski [13]) that (2.1) admits a unique solution and can be equivalently rewritten as the following variational inequality of the second kind

$$u \in H_0^1(\Omega): \quad a(u, v - u) + \phi(v) - \phi(u) \geq \ell(v - u), \quad v \in H_0^1(\Omega). \quad (2.6)$$

Let $\mathcal{T}$ be a given partition of Ω in triangles $t \in \mathcal{T}$. The sets of interior nodes and edges are called $\mathcal{N}$ and $\mathcal{E}$, respectively. Discretizing (2.6) by continuous,

piecewise linear finite elements $\mathcal{S} \subset H_0^1(\Omega)$, we obtain the finite dimensional problem

$$u_{\mathcal{S}} \in \mathcal{S} : \ a(u_{\mathcal{S}}, v - u_{\mathcal{S}}) + \phi_{\mathcal{S}}(v) - \phi_{\mathcal{S}}(u_{\mathcal{S}}) \geq \ell(v - u_{\mathcal{S}}), \ v \in \mathcal{S}. \qquad (2.7)$$

Observe that the functional ϕ is approximated by the $\mathcal{S}$–interpolation of the integrand $\Phi(v)$, giving

$$\phi_{\mathcal{S}}(v) = \int_\Omega \sum_{p \in \mathcal{N}} \Phi(v(p)) \lambda_p(x) dx, \qquad v \in \mathcal{S}, \qquad (2.8)$$

where $\Lambda = \{\lambda_p \mid p \in \mathcal{N}\}$ stands for the nodal basis of $\mathcal{S}$. Of course, the discrete problem (2.7) is uniquely solvable. For convergence results we refer for example to Brezzi et al. [6], Elliot [12] or Glowinski [13]. The efficient iterative solution of (2.7) by monotone multigrid methods has been considered by Kornhuber [18, 19].

3 Discrete Defect Problems

Assume that $\tilde{u} \in \mathcal{S}$ is an approximation of the finite element solution $u_{\mathcal{S}}$ of (2.7). In most applications $\tilde{u}$ is produced by some iterative solver. We want to derive upper and lower bounds for the *approximation error* $\|u - \tilde{u}\|$ with respect to the energy norm $\| \cdot \| = a(\cdot, \cdot)^{1/2}$. Note that the *algebraic error* $\|u_{\mathcal{S}} - \tilde{u}\|$ may interfere with the *discretization error* $\|u - u_{\mathcal{S}}\|$.

Observe that the desired defect $e = u - \tilde{u}$ is the unique solution of the defect problem

$$e \in H_0^1(\Omega) : \quad a(e, v - e) + \psi(v) - \psi(e) \geq r(v - e), \quad v \in H_0^1(\Omega), \quad (3.1)$$

where we have used the translated functional ψ defined by

$$\psi(v) = \phi(\tilde{u} + v) = \int_\Omega \Phi(\tilde{u}(x) + v(x))dx, \quad v \in H_0^1(\Omega),$$

and the residual

$$r = \ell - a(\tilde{u}, \cdot) \in H^{-1}(\Omega).$$

To discretize the continuous defect problem (3.1), we introduce the finite element space of continuous, piecewise quadratic functions $\mathcal{Q} \subset H_0^1(\Omega)$, spanned by the nodal basis

$$\Lambda_{\mathcal{Q}} = \{\lambda_p^{\mathcal{Q}} \mid p \in \mathcal{N}_{\mathcal{Q}}\}.$$

Here we have set $\mathcal{N}_{\mathcal{Q}} = \mathcal{N} \cup \mathcal{N}_{\mathcal{E}}$ and $\mathcal{N}_{\mathcal{E}}$ consists of the midpoints of the interior edges. Interpolating $\Phi(\tilde{u} + v)$ by piecewise quadratic finite elements, we obtain the approximation

$$\psi_{\mathcal{Q}}(v) = \int_\Omega \sum_{p \in \mathcal{N}_{\mathcal{Q}}} \Phi(\tilde{u}(p) + v(p))\lambda_p^{\mathcal{Q}}(x)dx, \quad v \in \mathcal{Q},$$

of the defect functional ψ. Then $e_{\mathcal{Q}} \in \mathcal{Q}$ is the unique solution of the *discrete defect problem*

$$e_{\mathcal{Q}} \in \mathcal{Q} : \quad a(e_{\mathcal{Q}}, v - e_{\mathcal{Q}}) + \psi_{\mathcal{Q}}(v) - \psi_{\mathcal{Q}}(e_{\mathcal{Q}}) \geq r(v - e_{\mathcal{Q}}), \quad v \in \mathcal{Q}. \quad (3.2)$$

There are other interesting ways of extending the underlying finite element space $\mathcal{S}$, in particular in the case of three space dimensions (see [5]). Correcting $\tilde{u}$ by $e_{\mathcal{Q}}$ we obtain the *piecewise quadratic approximation*

$$u_{\mathcal{Q}} = \tilde{u} + e_{\mathcal{Q}} \in \mathcal{Q}$$

with respect to the triangulation $\mathcal{T}$.

We now investigate the *effect of discretization* on the original defect problem.

Theorem 3.1 *Assume that u_Q provides a better approximation than $\tilde{u}$ in the sense that*

$$\|u - u_Q\| \le \beta \|u - \tilde{u}\| \qquad (3.3)$$

holds with some $\beta < 1$. Then we have the estimates

$$(1 + \beta)^{-1} \|e_Q\| \le \|u - \tilde{u}\| \le (1 - \beta)^{-1} \|e_Q\|. \qquad (3.4)$$

Proof. We only show the lower bound for $\|u - \tilde{u}\|$ which immediately follows from (3.3) and the triangle inequality

$$\|u - \tilde{u}\| \ge \|u_Q - \tilde{u}\| - \|u - u_Q\|.$$

∎

The crucial condition (3.3) with $\beta = \beta'\gamma < 1$ is a consequence of the *saturation assumption*

$$\|u - u_Q\| \le \beta' \|u - u_S\|, \quad \beta' < 1, \qquad (3.5)$$

and the *weakened best approximation property*

$$\|u - u_S\| \le \gamma \|u - \tilde{u}\|, \quad \gamma < 1/\beta'. \qquad (3.6)$$

The saturation assumption (3.5) states that the larger finite element space Q provides a better approximation than the original space S. In the case of elliptic selfadjoint problems, (3.5) is also a *necessary* condition for the upper estimate in (3.4) (c.f. [5]). For sufficiently regular problems the piecewise quadratic solution u_Q is even an approximation of higher order (see for instance [6]). In this case (3.5) clearly holds for sufficiently fine triangulations. On the other hand, there are simple examples showing that (3.5) may be violated, if the mesh is not properly chosen. In this sense reliable a posteriori error estimates still involve a certain amount of *a priori information*. See [5] for a detailed discussion.

Assuming that (3.5) is satisfied, the *accuracy assumption*

$$\|u_S - \tilde{u}\| \le \gamma' \|u - u_S\|, \quad 0 \le \gamma' < 1 - \beta',$$

implies the weakened best approximation property (3.6). For elliptic selfadjoint problems the condition (3.6) always holds with $\gamma = 1 < 1/\beta'$.

4 Preconditioned Discrete Defect Problems

In general, the solution of the discrete defect problem (2.7) is not available at reasonable computational cost. This motivates further simplifications, which should preserve the desired estimates (3.4).

Extending well–known results from the elliptic selfadjoint case [3, 4, 5, 9], we will now investigate the *effect of preconditioning* on the solution $e_\mathcal{Q}$ of (2.7). For this reason we consider the variational inequality

$$e_b \in \mathcal{Q}: \quad b(e_b, v - e_b) + \psi_\mathcal{Q}(v) - \psi_\mathcal{Q}(e_b) \geq r(v - e_b), \quad v \in \mathcal{Q}, \quad (4.1)$$

with some symmetric and positive definite bilinear form $b(\cdot, \cdot)$ on $\mathcal{Q}$. Observe that the *preconditioned defect problem* (4.1) is uniquely solvable and that the preconditioner $b(\cdot, \cdot)$ induces a norm $|\cdot| = b(\cdot, \cdot)^{1/2}$ on $\mathcal{Q}$.

Theorem 4.1 *Assume that the norm equivalence*

$$\gamma_0 b(v, v) \leq a(v, v) \leq \gamma_1 b(v, v), \quad v \in span\{e_\mathcal{Q}, e_b\}, \quad (4.2)$$

holds with nonnegative constants γ_0, γ_1. *Then we have the estimates*

$$(3\gamma_0^{-1} + 2)^{-1} |e_b|^2 \leq \|e_\mathcal{Q}\|^2 \leq (3\gamma_1 + 2)|e_b|^2. \quad (4.3)$$

Proof. By symmetry arguments it is sufficient to establish only the right inequality in (4.3). Inserting $v = e_b$ in the original discrete problem (2.7), some elementary calculations and (4.2) yield

$$\|e_\mathcal{Q}\|^2 \leq \gamma_1 |e_b|^2 + 2(\psi_\mathcal{Q}(e_b) - \psi_\mathcal{Q}(e_\mathcal{Q}) + r(e_\mathcal{Q} - e_b)). \quad (4.4)$$

The assertion now follows from

$$\psi_\mathcal{Q}(e_b) - \psi_\mathcal{Q}(e_\mathcal{Q}) + r(e_\mathcal{Q} - e_b) \leq (\gamma_1 + 1)|e_b|^2.$$

Inserting $v = e_\mathcal{Q}$ in (4.1) and using the Cauchy–Schwarz inequality, we get

$$\psi_\mathcal{Q}(e_b) - \psi_\mathcal{Q}(e_\mathcal{Q}) + r(e_\mathcal{Q} - e_b) \leq |e_b| |e_\mathcal{Q} - e_b|$$

so that it is sufficient to show

$$|e_\mathcal{Q} - e_b| \leq (1 + \gamma_1)|e_b|. \quad (4.5)$$

In order to prove (4.5), we insert $v = e_b$ in (3.2) and $v = e_\mathcal{Q}$ in the preconditioned problem (4.1). Adding the two resulting inequalities we obtain

$$a(e_\mathcal{Q}, e_b - e_\mathcal{Q}) + b(e_b, e_\mathcal{Q} - e_b) \geq 0$$

6

which can be reformulated as

$$|e_Q - e_b|^2 \leq b(e_Q, e_Q - e_b) - a(e_Q, e_Q - e_b).$$

The assertion now follows from the Cauchy–Schwarz inequality and (4.2). ∎

In the light of Theorem 4.1, we are left with the problem to select a preconditioner $b(\cdot, \cdot)$ which combines reasonable constants γ_0, γ_1 with a cheap evaluation of e_b. In analogy to the linear selfadjoint case one might be tempted to construct a preconditioner based on the hierarchical splitting

$$Q = S \oplus V \tag{4.6}$$

where the difference space $V = \mathrm{span}\{\lambda_p^Q \mid p \in \mathcal{N}_\mathcal{E}\}$ consists of the quadratic bubble functions associated with the edges $\mathcal{E}$ (c.f. [5, 9]).

However, in contrast to the linear case the unknowns now become coupled with respect to the functional ψ_Q as soon as the corresponding hierarchical basis is used. Even in simple cases, this coupling cannot be ignored without loosing the reliability of the resulting error estimate [16]. On the other hand, the global preconditioned problem is not solvable with reasonable computational effort.

To find a way out of this dilemma, observe that the constants γ_0, γ_1 appearing in the estimate (4.3) depend only on the *local quality* of the preconditioner $b(\cdot, \cdot)$ on the subspace span $\{e_Q, e_b\} \subset Q$. As a consequence, we can expect good results even from very simple preconditioners like the diagonal scaling

$$b(v, w) = \sum_{p \in \mathcal{N}_Q} v(p) w(p) a(\lambda_p^Q, \lambda_p^Q), \quad v, w \in Q, \tag{4.7}$$

if it is known a priori that e_Q and e_b are *high frequency* functions.

Moreover, the preconditioned defect equation (4.1) resulting from the diagonal scaling (4.7) can be decomposed in separate *local subproblems* for the nodal values of e_b. For piecewise quadratic scalar functions Φ these sub–problems can be solved explicitly.

This heuristic approach can be justified in the special case of linear elliptic problems.

Proposition 4.1 *Let the preconditioner $b(\cdot, \cdot)$ be given by (4.7). Assume that $\Phi \equiv 0$ and that the discrete problem (2.7) has been solved exactly, i.e. $\tilde{u} = u_S$. Then the estimates (4.3) hold with constants depending only on the ellipticity of $a(\cdot, \cdot)$ and on the shape regularity of $\mathcal{T}$.*

Proof. Let us consider the hierarchical splitting (4.6). For some given $v \in Q$ the superscripts S and V will indicate the contributions $v^S \in S$ and

$v^{\mathcal{V}} \in \mathcal{V}$ of the unique decomposition $v = v^{\mathcal{S}} + v^{\mathcal{V}}$. We will make use of the bilinear forms

$$\hat{a}(v,w) = a(v^{\mathcal{S}}, v^{\mathcal{S}}) + \sum_{p \in \mathcal{N}_{\mathcal{E}}} v^{\mathcal{V}}(p) w^{\mathcal{V}}(p) a(\lambda_p^{\mathcal{Q}}, \lambda_p^{\mathcal{Q}})$$

and

$$\hat{b}(v,w) = \sum_{p \in \mathcal{N}} v^{\mathcal{S}}(p) w^{\mathcal{S}}(p) a(\lambda_p^{\mathcal{Q}}, \lambda_p^{\mathcal{Q}}) + \sum_{p \in \mathcal{N}_{\mathcal{E}}} v^{\mathcal{V}}(p) w^{\mathcal{V}}(p) a(\lambda_p^{\mathcal{Q}}, \lambda_p^{\mathcal{Q}})$$

defined on $\mathcal{Q}$. Observe that both preconditioners are based on the hierarchical splitting (4.6) and subsequent diagonalization. Using the standard affine transformation technique in a similar way as for example in [5, 9], it can be shown that the norm equivalences

$$b(v,v) \asymp \hat{b}(v,v), \qquad \hat{a}(v,v) \asymp a(v,v) \tag{4.8}$$

hold for all $v \in \mathcal{Q}$. Here the abbreviation $x \asymp y$ stands for the estimates $cy \le x \le Cy$ with constants c, C depending only on the ellipticity of $a(\cdot,\cdot)$ and on the shape regularity of $\mathcal{T}$. Using the preconditioners $\hat{a}(\cdot,\cdot)$ and $\hat{b}(\cdot,\cdot)$ in the preconditioned defect problem (4.1), we obtain the corrections $e_{\hat{a}}$ and $e_{\hat{b}}$, respectively. Now the estimates

$$|e_b|^2 \asymp \hat{b}(e_{\hat{b}}, e_{\hat{b}}), \qquad \hat{a}(e_{\hat{a}}, e_{\hat{a}}) \asymp \|e_{\mathcal{Q}}\|^2 \tag{4.9}$$

are an immediate consequence of Theorem 4.1. The crucial question is how to relate $\hat{b}(e_{\hat{b}}, e_{\hat{b}})$ to $\hat{a}(e_{\hat{a}}, e_{\hat{a}})$.

Here we make heavily use of the assumption $\Phi \equiv 0$. In this case the defect problem (3.2) reduces to the variational equality

$$e_{\mathcal{Q}} \in \mathcal{Q}: \qquad a(e_{\mathcal{Q}}, v) = r(v), \qquad v \in \mathcal{Q}. \tag{4.10}$$

Replacing $a(\cdot,\cdot)$ by the preconditioner $\hat{b}(\cdot,\cdot)$, the linear and the quadratic contribution of $e_{\hat{b}} = e_{\hat{b}}^{\mathcal{S}} + e_{\hat{b}}^{\mathcal{V}}$ are completely decoupled. The same happens if the other hierarchical preconditioner $\hat{a}(\cdot,\cdot)$ is used. Applying in addition that $r(v) = 0$ holds for all $v \in \mathcal{S}$ (a consequence of the second assumption $\tilde{u} = u_{\mathcal{S}}$), we get

$$e_{\hat{b}}^{\mathcal{S}} = e_{\hat{a}}^{\mathcal{S}} = 0, \qquad e_{\hat{b}}^{\mathcal{V}} = e_{\hat{a}}^{\mathcal{V}}. \tag{4.11}$$

This clearly yields $\hat{b}(e_{\hat{b}}, e_{\hat{b}}) = \hat{a}(e_{\hat{a}}, e_{\hat{a}})$ and the assertion follows from (4.9). ∎

Proposition 4.1 can be extended to variational inequalities under severe restrictions on the behavior of the discrete free boundary (see [20]). The main difficulty is that the equations (4.11) are no longer valid because now the linear and the quadratic parts of $e_{\hat{b}}$ and $e_{\hat{a}}$ *remain coupled* with respect to the nonlinear functional $\psi_{\mathcal{Q}}$. This is the same problem as mentioned above.

Nevertheless Proposition 4.1 gives some motivation to assume that the correction e_Q is a high frequency function. Then Theorem 4.1 assures that $|e_b|$ provides reasonable lower and upper bounds for the exact correction $\|e_Q\|$. This heuristic reasoning is strengthened by our numerical experiments reported below. Recall that there are no such results for the comparable local error estimate considered in [16, 22].

To increase the robustness (and unfortunately the computational costs) of the a posteriori error estimation we may consider the following iterative scheme

$$e^{\nu+1} = e^\nu + \mathcal{B}(e^\nu), \quad \nu = 0, 1, \ldots, \quad e^0 = 0, \tag{4.12}$$

where $\mathcal{B}$ is intended to generalize the role of a preconditioner to nonlinear problems. In this case, the resulting error estimate $\|e^1\|$ depends on the convergence rates of the iteration (4.12). We refer to [20] for further information.

5 Numerical Experiments

A posteriori estimates are typically used as part of an adaptive multilevel method in order to provide stopping criteria for the complete algorithm and local error indicators for the adaptive refinement. Based on the *global* estimate $|e_b|$ as resulting from (4.1) with diagonal scaling (4.7) we select *local* error indicators as follows.

Using the hierarchical splitting (4.6) we decompose e_b according to

$$e_b = e_b^{\mathcal{S}} + e_b^{\mathcal{V}}, \quad e_b^{\mathcal{S}} \in \mathcal{S}, \quad e_b^{\mathcal{V}} \in \mathcal{V}.$$

Here $e_b^{\mathcal{S}}$ and $e_b^{\mathcal{V}}$ represent the low and high frequency parts of e_b. In analogy to the linear selfadjoint case we want to refine the given triangulation $\mathcal{T}$ in such regions where the high frequency contributions deteriorate the overall accuracy. Hence, the local contributions η_p,

$$\eta_p = e_b^{\mathcal{V}}(p)^2 a(\lambda_p^{\mathcal{Q}}, \lambda_p^{\mathcal{Q}}), \quad p \in \mathcal{N}_{\mathcal{E}},$$

of $|e_b^{\mathcal{V}}|^2 = \sum_{p \in \mathcal{N}_{\mathcal{E}}} \eta_p$ are used as *local error indicators*. If η_p exceeds a certain threshold $\bar{\eta}$ then the two triangles containing p are marked for refinement. The threshold $\bar{\eta}$ is computed by extrapolation [1]. Marked triangles are subdivided into four congruent subtriangles. Additional refinement may be necessary for structural reasons. See for example Bank [2] or Deuflhard, Leinen and Yserentant [9] for further information.

An *adaptive cycle* consists of discretization, iterative solution and adaptive refinement of the given triangulation. An adaptive algorithm is producing a sequence of triangulations $\mathcal{T}_j$, of corresponding approximations $\tilde{u}_j$ and of error estimates $|e_b^j|$, $j = 0, \ldots$, by inductive application of adaptive cycles to an intentionally coarse initial triangulation $\mathcal{T}_0$. The algorithm stops if the estimated error is bounded by some prescribed accuracy TOL,

$$|e_b^j| \leq \text{TOL}. \tag{5.1}$$

The *refinement level* j counts the number of adaptive cycles while the *refinement depth* of $\mathcal{T}_j$ denotes the maximal number of successive refinements applied to an initial triangle $t \in \mathcal{T}_0$. For selfadjoint elliptic problems a theoretical justification of the described adaptive approach was recently given by Dörfler [10].

In the following numerical examples, we always require an estimated accuracy of 5.%. More precisely, the computation is stopped if (5.1) is satisfied with $\text{TOL} = 0.05 \cdot \|\tilde{u}_j\|$. The approximate solutions $\tilde{u}_j$ of the discrete problems (2.7) are computed up to an accuracy of 0.5% using monotone multigrid methods as introduced by Kornhuber [18, 19]. The implementation was carried out in the framework of a recent C++ version of the finite element toolbox KASKADE.

Example 5.1: Obstacle Problem   We consider the numerical solution of the obstacle problem

$$u \in \mathcal{K}: \qquad \mathcal{J}(u) \le \mathcal{J}(v), \qquad v \in \mathcal{K}, \tag{5.2}$$

where $\mathcal{J}$ is defined in (2.2) and the closed convex set $\mathcal{K}$ is given by

$$\mathcal{K} = \{v \in H_0^1(\Omega) \mid v(x) \le \varphi(x) \text{ a.e. in } \Omega\}$$

with some obstacle function $\varphi \in H_0^1(\Omega)$. It is easily checked that (5.2) can be rewritten in the form of our general problem (2.1) with the scalar function Φ given by (2.4).

In our numerical computations we select the quadratic form $a(\cdot, \cdot)$ and the right hand side $\ell(\cdot)$ according to

$$a(v, w) = \int_\Omega \partial_1 v \partial_1 w + \partial_2 v \partial_2 w \, dx, \quad \ell(v) = 2C \int_\Omega v \, dx$$

and the obstacle function is given by $\varphi(x) = \text{dist}(x, \partial\Omega)$, $x \in \Omega$. Finally let $\Omega = (0,1) \times (0,1)$.

The resulting obstacle problem (5.2) is modeling the elasto–plastic torsion of a cylindrical bar with cross–section Ω. The active points (where $u(x) = \text{dist}(x, \partial\Omega)$) characterize the plastic region, while the material is considered elastic in inactive points. The solution u represents the stress potential and the applied twist angle is expressed by the parameter C. We refer for example to Rodrigues [26] for further information.

The inactive region is located along the diagonals of Ω and becomes arbitrarily small with increasing C. This leads to various numerical difficulties so that (5.2) has become a well–established test example [13, 14, 15, 16, 18, 23]. Following [16], we chose the parameter $C = 15$ and the initial triangulation $\mathcal{T}_0$ as depicted in Figure 5.1.

Starting with $\mathcal{T}_0$, our adaptive algorithm generates a sequence of successively refined triangulations $\mathcal{T}_0, \dots, \mathcal{T}_9$ and of corresponding approximations $\tilde{u}_0, \dots, \tilde{u}_9$. The final triangulation $\mathcal{T}_9$ is depicted in the left picture of Figure 5.2. The right picture shows the (discrete) free boundary of the final approximation $\tilde{u}_9$. Observe that $\mathcal{T}_9$ is almost uniformly refined in the inactive region and as coarse as possible in the remaining part of Ω. As the solution is smooth and the (piecewise linear) obstacle is represented exactly by the finite element approximations, this triangulation is well–suited to the actual problem. The very thin inactive region has no adequate representation on the coarse grids. Even if $\mathcal{T}_0$ is uniformly refined, all nodal points remain active up to the 3rd refinement level. Hence, the detection and location of the inactive region is a quite challenging task for an adaptive scheme.

11
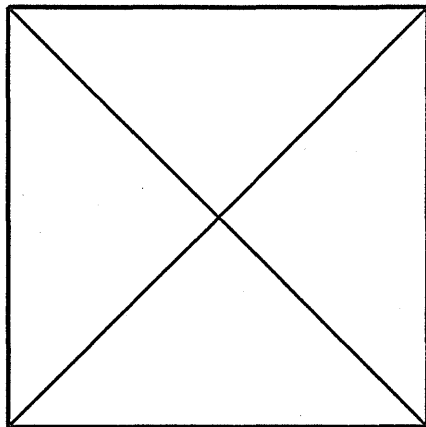
Figure 5.1: Initial Triangulation $\mathcal{T}_0$
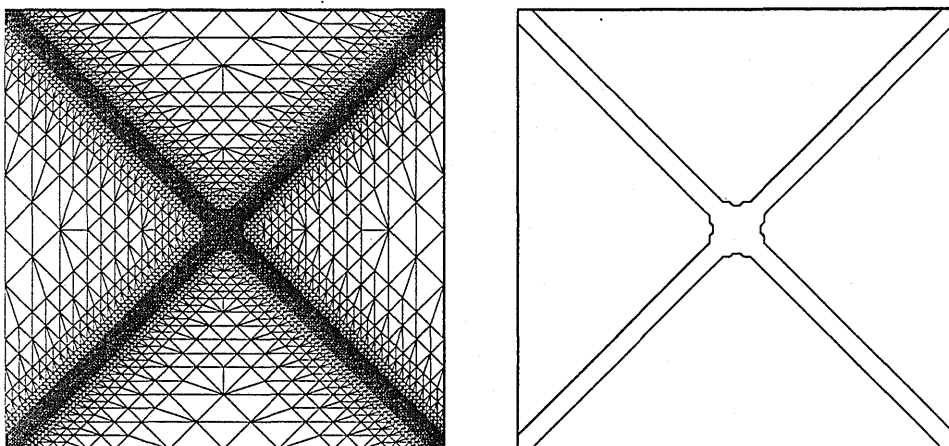
Figure 5.2: Final Triangulation $\mathcal{T}_9$ and Approximate Free Boundary

To check the quality of the global error estimate $|e_b^j|$ on each refinement level $j = 0, \dots, 9$, we consider the *effectivity index* κ_j

$$\kappa_j = |e_b^j| / \|u - \tilde{u}_j\|, \quad j = 1, \dots, 9. \tag{5.3}$$

A computable approximation of κ_j is obtained by replacing the exact solution u by the approximation resulting from two further uniform refinements of the final triangulation $\mathcal{T}_9$.

The complete refinement history is reported in Table 1.

Level	Depth	Nodes	est. Error	Effectivity
0	0	1	38.4 %	2.53
1	1	5	38.4 %	2.53
2	2	13	27.4 %	1.80
3	3	53	21.8 % ·	1.51
4	4	93	17.8 %	1.24
5	5	277	13.4 %	1.02
6	5	357	12.8 %	1.02
7	5	713	10.8 %	1.52
8	6	1577	5.4 %	1.61
9	7	5905	2.8 %	1.69

Table 1. Refinement History

Observe that the resulting effectivity indices can be interpreted as

$$0.4|e_b^j| \leq \|u - \tilde{u}_j\| \leq |e_b^j|, \qquad j = 0, \ldots, 9,$$

with even better results on the fine levels. Hence, our error estimate works satisfactory throughout the approximation. A comparable a posteriori error estimate [16, 21, 22] fails for this example. More precisely, this estimator does not detect the inactive region so that it simply provides the error estimate zero on the first levels. It is interesting that the refinement history is very similar as in [16] where a considerably more expensive semi–local error estimate has been used.

Example 5.2: A Semidiscrete Stefan Problem   The nonlinear evolution equation

$$\tfrac{\partial}{\partial t}\mathcal{H}(U) - \Delta U = F, \quad \text{in } \Omega \times (0, T), \qquad (5.4)$$

with suitable initial and boundary conditions describes the heat conduction in Ω undergoing a change of phase. F is a body heating term and the generalized enthalpy $\mathcal{H}$ is a scalar maximal monotone multifunction,

$$\mathcal{H}(z) = \begin{cases} c_1(z - \theta_0)k_1 & \text{if } z < \theta_0 \\ [0, L] & \text{if } z = \theta_0, \\ c_2(z - \theta_0)/k_2 + L & \text{if } z > \theta_0 \end{cases} \quad z \in \mathbb{R}, \qquad (5.5)$$

which is set–valued at the phase change temperature θ_0. The unknown generalized temperature U is resulting from the standard Kirchhoff transformation $U = k_1\theta$ for $\theta < \theta_0$ and $U = k_2\theta$ for $U > \theta_0$ of the physical temperature θ. The positive constants c_i, k_i, $i = 1, 2$, describe the thermal properties in the two different phases and $L > 0$ stands for the latent heat.

13

Discretizing (5.4) in time by the backward Euler scheme with respect to some step size $\tau > 0$, the spatial problems at the different time levels $t_k = k\tau$ can be identified with problems of the form (2.1). The solution $u = U_\tau(\cdot, t_k)$ is the approximation at the actual time step, the bilinear form $a(v, w) = \tau(\nabla v, \nabla w)$ is generated by the Laplacian and the functional ℓ is given by $\ell(v) = (\tau F_k + H_{k-1}, v)$ with $F_k = F(\cdot, t_k)$ and an appropriate selection $H_{k-1} \in \mathcal{H}(U_\tau(\cdot, t_{k-1}))$. The convex, scalar function Φ is chosen in such a way that $\mathcal{H} = \partial\Phi$ is the subdifferential of Φ. Note that Φ is a piecewise quadratic function of the form (2.5). This semi–discretization has been used to establish existence and uniqueness of a weak solution U (see for example Jerome [17]) and also provides a general framework for a variety of numerical methods.

Adaptive techniques for the two–phase Stefan problem have been derived by Nochetto, Paolini and Verdi [24, 25]. In contrast to our approach which is aiming at the adaptive solution of the spatial problems up to a certain accuracy, their local error indicators concentrate exclusively on an efficient resolution of the free boundary.

We will consider a model problem due to Ciavaldini [7]. The space–time domain $\Omega \times (0, T)$ is given by $\Omega = (0, 1) \times (0, 1)$ and $T = 0.5$. The physical data are $c_1 = 2$, $k_1 = 1$, $c_2 = 6$, $k_2 = 2$ and $\theta_0 = 0$, $L = 1$. Using the right hand side

$$F(x, t) = \begin{cases} c_1 exp(-4t) - 4k_1 & \text{if } \theta < 0 \\ c_2 exp(-4t) - 4k_2 & \text{if } \theta > 0 \end{cases}, \quad x \in \Omega, \, t > 0,$$

the Kirchhoff transform U of the physical temperature θ given by

$$\theta(x_1, x_2, t) = (x_1 - 0.5)^2 + (x_2 - 0.5)^2 - exp(-4t)/4, \quad (x_1, x_2) \in \Omega, t \geq 0,$$

is the exact solution of (5.4) with the corresponding initial and boundary conditions. For the semi-discretization we choose the uniform time step $\tau = 0.0125$.

Recall that an estimated accuracy of 5.% is required on each time level. We always start with initial triangulation $\mathcal{T}_0$ as shown in Figure 1.

The evolution of the solution is shown in Figure 5.3 showing the discrete interface and the approximate physical solution along the diagonal $x_1 = x_2$ for the first and the last time step. The corresponding final triangulations are depicted in Figure 5.4. In both cases the refinement concentrates on the lack of regularity at the interface.
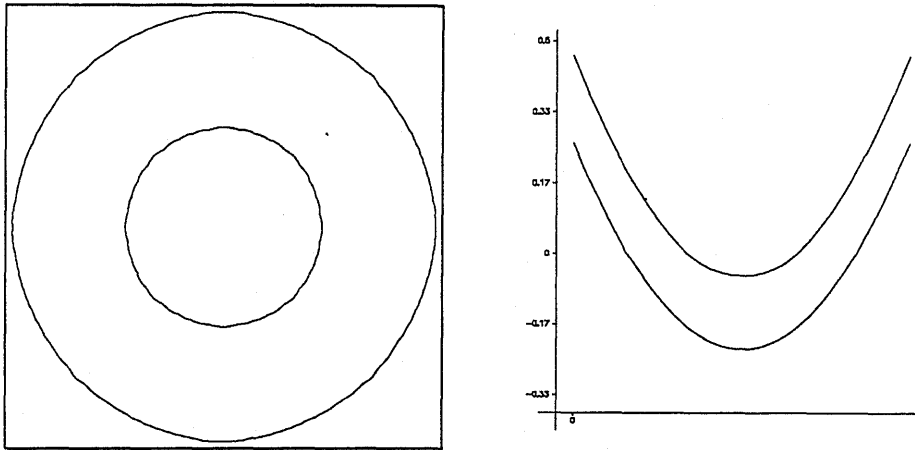
Figure 5.3: Discrete Interfaces and Diagonal Cuts for the First and the Last Time Step
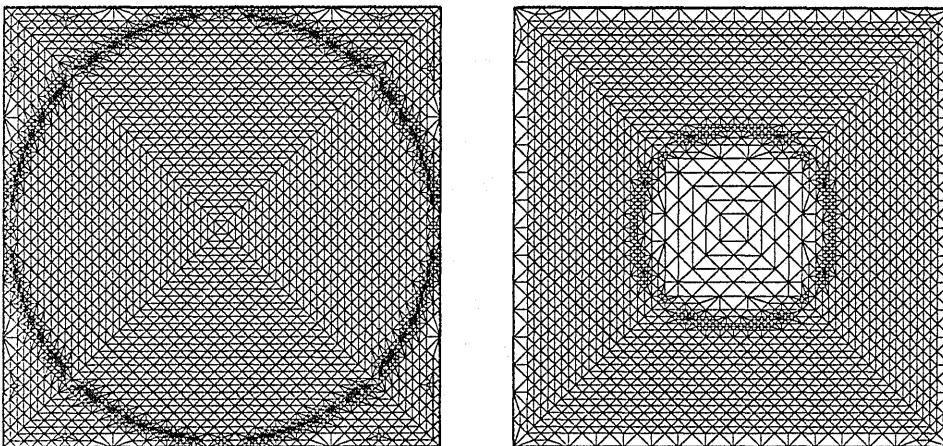
Figure 5.4: Final Triangulations for the First and the Last Time Step

The complete refinement history for the first time step is given in Table 2 where the effectivity rates are computed according to (5.3). On the subsequent time levels we found similar results.

Level	Depth	Nodes	est. Error	Effectivity
0	0	1	1.6e2 %	0.14
1	1	5	1.9e2 %	0.65
2	2	25	1.9e2 %	2.0
3	3	65	56.8 %	0.80
4	4	261	36.7 %	1.76
5	5	409	24.0 %	0.96
6	5	517	17.2 %	0.84
7	6	717	13.1 %	0.90
8	7	1225	7.9 %	0.62
9	7	1629	6.9 %	0.98
10	7	2133	5.9 %	1.04
11	7	3149	4.4 %	0.92

Table 2. History for the First Time Step

As in the previous example the results show a similar efficiency and reliability as for related linear selfadjoint problems.

Bibliography

[1] I. Babuška and W.C. Rheinboldt. Error estimates for adaptive finite element computations. *SIAM J. Numer. Anal.*, 15:736–754, 1978.

[2] R.E. Bank. *PLTMG – A Software Package for Solving Elliptic Partial Differential Equations, User's Guide 6.0*. Frontiers in Applied Mathematics. SIAM, Philadelphia, 1990.

[3] R.E. Bank and R.K. Smith. A posteriori error estimates based on hierarchical bases. *SIAM J. Num. Anal.*, 30:921–935, 1993.

[4] F.A. Bornemann, B. Erdmann, and R. Kornhuber. Adaptive multilevel methods in three space dimensions. *J. Numer. Meth. Engrg.*, 36:3187–3203, 1993.

[5] F.A. Bornemann, B. Erdmann, and R. Kornhuber. A posteriori error estimates for elliptic problems in two and three space dimensions. *SIAM J. Numer. Anal.*, to appear.

[6] F. Brezzi, W.W. Hager, and P.A. Raviart. Error estimates for the finite element solution of variational inequalities I. *Numer. Math.*, 28:431–443, 1977.

[7] J.F. Ciavaldini. Analyse numérique d'un problème de Stefan a deux phases par une méthode d'éléments finis. *SIAM J.Numer.Anal.*, 12:464–487, 1975.

[8] J. Crank. *Free and Moving Boundary Problems*. Oxford University Press, Oxford, 1988.

[9] P. Deuflhard, P. Leinen, and H. Yserentant. Concepts of an adaptive hierarchical finite element code. *IMPACT Comput. Sci. Engrg.*, 1:3–35, 1989.

[10] W. Dörfler. Orthogonale fehlermethoden. Manuscript, 1993.

[11] G. Duvaut and J.L. Lions. *Les inéquations en mécanique et en physique*. Dunaud, Paris, 1972.

[12] C.M. Elliot. Error analysis of the enthalpy method for the Stefan problem. *IMA J. Numer. Anal.*, 7:61–71, 1987.

[13] R. Glowinski. *Numerical Methods for Nonlinear Variational Problems*. Springer-Verlag, New York, 1984.

[14] R. Glowinski, J.L. Lions, and Trémolières. *Numerical Analysis of Variational Inequalities*. North–Holland, Amsterdam, 1981.

[15] R.H.W. Hoppe. Multigrid algorithms for variational inequalities. *SIAM J. Numer. Anal.*, 24:1046–1065, 1987.

[16] R.H.W. Hoppe and R. Kornhuber. Adaptive multilevel–methods for obstacle problems. *SIAM J. Numer. Anal.*, 31(2):301–323, 1994.

[17] J.W. Jerome. *Approximation of Nonlinear Evolution Equations*. Academic Press, New York, 1983.

[18] R. Kornhuber. Monotone multigrid methods for elliptic variational inequalities I. *Numer. Math.*, to appear.

[19] R. Kornhuber. Monotone multigrid methods for elliptic variational inequalities II. *Numer. Math.*, submitted.

[20] R. Kornhuber. Adaptive monotone multigrid methods for nonlinear variational problems. Habilitationsschrift, FU Berlin, 1995.

[21] R. Kornhuber and R. Roitzsch. Self adaptive computation of the breakdown voltage of planar pn–junctions with multistep field plates. In Fichtner W. and Aemmer D., editors, *Simulation of Semiconductor Devices and Processes*, pages 535–543, Konstanz, 1991. Hartung–Gorre.

[22] R. Kornhuber and R. Roitzsch. Self adaptive finite element simulation of bipolar, strongly reverse biased pn-junctions. *Comm. Num. Meth. in Engrg.*, 9:243–250, 1993.

[23] Y. Kuznetsov, P. Neittaanmäki, and P. Tarvainen. Overlapping block relaxation and schwarz methods for the obstacle problem with a convection diffusion operator. Technical Report Report 4/1993, University of Jyväskylä, 1993.

[24] R. H. Nocchetto, M. Paolini, and C. Verdi. An adaptive finite element method for two–phase Stefan problems in two space dimensions. Part I Stability and error estimates. *Math. Comp.*, 57(195):73–108, 1991.

[25] R. H. Nocchetto, M. Paolini, and C. Verdi. An adaptive finite element method for two–phase Stefan problems in two space dimensions. Part II Implementation and numerical experiments. *SIAM J. Sci. Stat. Comput.*, 12(5):1207–1244, 1991.

[26] J.F. Rodrigues. *Obstacle Problems in Mathematical Physics*. Number 134 in Mathematical Studies. North–Holland, Amsterdam, 1987.

[27] R. Verfürth. A review of a posteriori error estimation and adaptive mesh–refinement techniques. Manuscript, 1993.

[28] R. Verfürth. A posteriori error estimation and adaptive mesh–refinement techniques. *J. Comp. Appl. Math.*, 50:67–83, 1994.

[29] O.C. Zienkiewicz, J.P. De S.R. Gago, and D.W. Kelly. The hierarchical concept in finite element analysis. *Computers & Structures*, 16:53–65, 1983.

Recent publications of the
Weierstraß–Institut für Angewandte Analysis und Stochastik

Preprints 1994

112. Henri Schurz: A note on pathwise approximation of stationary Ornstein–Uhlenbeck processes with diagonalizable drift.

113. Peter Mathé: On the existence of unbiased Monte Carlo estimators.

114. Kathrin Bühring: A quadrature method for the hypersingular integral equation on an interval.

115. Gerhard Häckl, Klaus R. Schneider: Controllability near Takens–Bogdanov points.

116. Tatjana A. Averina, Sergey S. Artemiev, Henri Schurz: Simulation of stochastic auto–oscillating systems through variable stepsize algorithms with small noise.

117. Joachim Förste: Zum Einfluß der Wärmeleitung und der Ladungsträgerdiffusion auf das Verhalten eines Halbleiterlasers.

118. Herbert Gajewski, Konrad Gröger: Reaction–diffusion processes of electrically charged species.

119. Johannes Elschner, Siegfried Prössdorf, Ian H. Sloan: The qualocation method for Symm's integral equation on a polygon.

120. Sergej Rjasanow, Wolfgang Wagner: A stochastic weighted particle method for the Boltzmann equation.

121. Ion G. Grama: On moderate deviations for martingales.

122. Klaus Fleischmann, Andreas Greven: Time–space analysis of the cluster–formation in interacting diffusions.

123. Grigori N. Milstein, Michael V. Tret'yakov: Weak approximation for stochastic differential equations with small noises.

124. Günter Albinus: Nonlinear Galerkin methods for evolution equations with Lipschitz continuous strongly monotone operators.

125. Andreas Rathsfeld: Error estimates and extrapolation for the numerical solution of Mellin convolution equations.

126. Mikhail S. Ermakov: On lower bounds of the moderate and Cramer type large deviation probabilities in statistical inference.

127. Pierluigi Colli, Jürgen Sprekels: Stefan problems and the Penrose–Fife phase field model.

128. Mikhail S. Ermakov: On asymptotic minimaxity of Kolmogorov and omega-square tests.

129. Gunther Schmidt, Boris N. Khoromskij: Boundary integral equations for the biharmonic Dirichlet problem on nonsmooth domains.

130. Hans Babovsky: An inverse model problem in kinetic theory.

131. Dietmar Hömberg: Irreversible phase transitions in steel.

132. Hans Günter Bothe: How 1–dimensional hyperbolic attractors determine their basins.

133. Ingo Bremer: Waveform iteration and one–sided Lipschitz conditions.

134. Herbert Gajewski, Klaus Zacharias: A mathematical model of emulsion polymerization.

135. J. Theodore Cox, Klaus Fleischmann, Andreas Greven: Comparison of interacting diffusions and an application to their ergodic theory.

136. Andreas Juhl: Secondary Euler characteristics of locally symmetric spaces. Results and Conjectures.

137. Nikolai N. Nefedov, Klaus R. Schneider, Andreas Schuppert: Jumping behavior in singularly perturbed systems modelling bimolecular reactions.

138. Roger Tribe, Wolfgang Wagner: Asymptotic properties of stochastic particle systems with Boltzmann type interaction.

Preprints 1995

139. Werner Horn, Jan Sokolowski, Jürgen Sprekels: Control problems with state constraints for the Penrose–Fife phase-field model.

140. Hans Babovsky: Simulation of kinetic boundary layers.